RSC Advances

ROYAL SOCIETY OF CHEMISTRY

www.rsc.org/advances

Journal Name

Dynamic Article Links ►

Cite this: DOI: 10.1039/c0xx00000x

www.rsc.org/xxxxxx

ARTICLE TYPE

A novel coumarin based molecular switch for dual sensing of Zn(II) and Cu(II)

Deblina Sarkar, Ajoy Kumar Pramanik, and Tapan Kumar Mondal*

An efficient coumarin based molecular switch for the dual sensing of two environmentally as well as biologically important cations Zn^{2+} and Cu^{2+} has been synthesized. The receptor H_2L shows about 6 fold enhancement in fluorescent intensity upon addition of Zn^{2+} and also exhibits quenching of emission intensity upon addition of Cu^{2+} without the interference of other metal ions present in solution. In case of other metal ions no significant change in emission intensity is observed. H_2L presents a tunable system comprising of two INHIBIT logic gates with Zn^{2+} and Cu^{2+} or Zn^{2+} and EDTA as chemical inputs by monitoring the emission mode. An IMPLICATION logic gate is obtained with Cu^{2+} and EDTA as chemical inputs and emission as the output mode.

Introduction

Zinc(II) and copper(II) plays a very crucial role in the human body and serves as the second and third most abundant transition metal ions after iron(III), found in the human body.[1] Highest concentration of zinc in the human body is found in the brain and plays an important role in many biological processes such as regulation of gene expressions, apoptosis, neural signal transmitters and catalytic cofactors.[2] However metabolic disorders of zinc(II) leads to several neurodegenerative diseases such as Parkinson's and Alzheimer's diseases.[3] Again, inadequate level of zinc leads to retardation of growth, decrease in the immunological defense, eye lesion and some skin diseases.[4] Copper(II) also plays a significant role in biological, environmental and chemical systems.[5] The disorder in Cu(II) metabolism may lead to severe diseases, such as Alzheimer's and Wilson's diseases, amyotrophic lateral sclerosis, Menkes syndrome and haematological manifestations.[6-11] Thus detection of zinc(II) and copper(II) is of utmost importance from both environmental as well as biological point of views.

Development of artificial chemosensors based on fluorescence technique has emerged out to be a powerful detection tool owing to its simplicity, sensitivity and tunability.[12] In few recent years, several small molecules for the detection of zinc(II),[13] by the enhancement of fluorescent intensity have been reported while several reported molecules have the capability to detect copper by quenching of fluorescent intensity.[14] Most of the reported chemosensors for zinc suffer the problem of interference from Cd^{2+} because of similarity in the electronic configuration.[15] Till date only a few chemosensors with dual sensing properties for metal ions have been reported.[16] Thus the development of dual chemosensors for the detection of vital elements still remains an active field of research.

Development of various chemical systems to exhibit operations such as AND, OR, NOT and their integrated operations have been carried out.[17] Small molecules with more than one output channel are of utmost interest as they form the basis of molecular logic gates capable of performing several arithmetic operations.[18] Various single molecules have been exploited for the construction of many useful integrated logic gates such as INHIBIT, half subtractor, half adder, full adder, and full subtractor.[19] However very few IMPLICATION gates have been reported so far.[20] Recently L. Zhao *et.al* has reported several molecular logic gates based on salicylidine Schiff base.[21] In our previous work we have reported an INHIBIT logic gate based on a coumarin Schiff base with Al^{3+} and EDTA as chemical inputs.[22]

In this present work we have reported the synthesis and spectral characterizations of a coumarin based organic framework which has the dual sensing property for zinc(II) and copper(II) by subsequent enhancement and quenching of fluorescence intensity. Coumarin framework exhibits various interesting photophysical properties such as Stokes shift and visible excitation and emission wavelengths, and also has high importance as fluorescent dyes.[23] Only a few coumarin based chemosensors are reported so far for the dual sensing of metal ions.[24] Till date, there has been no report of coumarin based chemosensor for dual sensing of Zn^{2+} and Cu^{2+}. Only a few reported chemosensors are known to selectively recognize these two vital elements zinc and copper. S. Wang et al. has reported a binaphthyl-derived salicylidene Schiff base for dual sensing of Cu(II) and Zn(II).[25] Y. Liu et al. has reported a fluorescent 'off-on-off' probe for relay recognition of Zn^{2+} and Cu^{2+} derived from N,N-bis(2-pyridylmethyl)amine[26] while L. Qua et al. has recently reported a pyridoxal-based dual chemosensor for zinc and copper.[27] However, most of these reported chemosensors have lower binding constants for Zn^{2+} and Cu^{2+} and also higher limit of detection, compared to that of our newly developed receptor H_2L. In certain cases, the receptor is synthesized using several steps along with the use of reagents which are difficult to handle. Whereas in the present case, the synthetic route towards H_2L is very facile and economically cheap. The developed chemosensor is highly efficient in the detection of zinc(II) with enhancement of fluorescence intensity by 6 fold while it detects copper by quenching of emission intensity, by 7 folds. H_2L presents a tunable system comprising of two INHIBIT logic gates with Zn^{2+} and Cu^{2+} or Zn^{2+} and EDTA as chemical inputs. An IMPLICATION logic gate is obtained with Cu^{2+} and EDTA as chemical inputs and emission as the output mode. H_2L exhibits very high selectivity only for copper and zinc with no interference from any other metal ions including cadmium. Thus the synthesized chemosensor H_2L is an important addition to the list of few reported simple organic molecules which can detect zinc and copper selectively.

Results and discussion

Synthesis and spectral characterisation

Synthetic route towards H_2L involves a very facile and economically cheap route using Schiff base condensation of 3-acetyl-4-hydroxycoumarin with p-Phenylenediamine in 2:1 molar ratio in methanolic medium under refluxing condition for 6 hours. (Scheme 1).

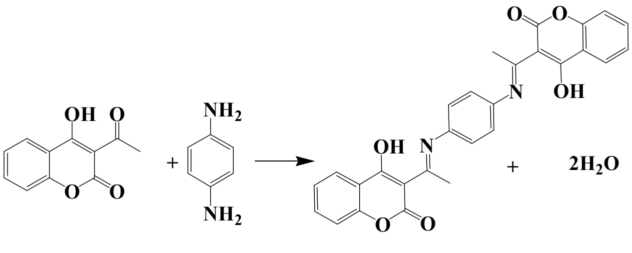

H_2L

Scheme 1. Synthesis of chemosensor H_2L

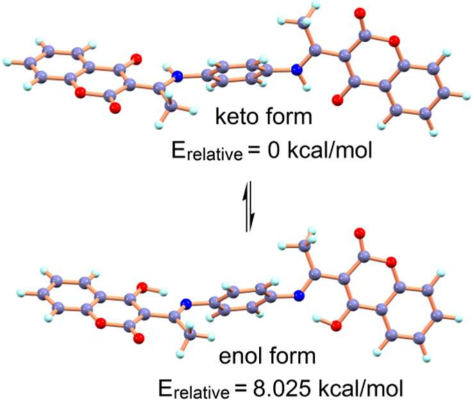

Scheme 2. Keto-enol tautomerism of H_2L and their relative energies calculated by DFT/B3LYP/6-31G(d,p) method

The ligand H_2L may exist in equilibrium in the keto and enol form by excited state intramolecular proton transfer process (ESIPT) which is further supported by the small energy gap (ΔE = 8.025 kcal/mol) between the two tautomeric forms (Scheme 2). The energies calculated by DFT/B3LYP/6-31G(d,p) method indicate that the keto form is more stable than the enol form by 8.025 kcal/mol. IR spectrum of H_2L taken in KBr disk shows a stretching band at 1698 cm^{-1} corresponding to lactone C=O, the keto C=O and C=C appears at 1610 cm^{-1} and 1547 cm^{-1} respectively (Fig. S1). ^1H-NMR spectra are recorded in $CDCl_3$ which shows a band at around δ 15.45 which is due to the hydrogen bonded NH proton (Fig. S4). This peak vanishes in the H_2L-Zn^{2+} complex indicating co-ordination to the metal centre through N donating site of the enol form (Fig. S5). The aromatic protons in H_2L appear as expected in the region δ 8.10-7.27. The -N=C(CH_3)- protons appear at δ 2.79 as singlet. All aromatic protons appear at a bit downfield position compared to that of H_2L, which can clearly be explained due to the co-ordination of Zn^{2+} with H_2L. However, the coordination of H_2L with Cu^{2+} could not be studied by NMR spectroscopy owing to the paramagnetic nature of Cu^{2+} ion. Mass spectrum shows m/z peak corresponding to $H^+[H_2L]$ at 481.2 for H_2L (Fig. S6). For H_2L-Zn^{2+} complex the strong peak at 703.3 correspond to $Na[Zn_2(L)Cl_2]^+$ along with a weak peak at 739.4 corresponding to $Na[Zn_2(L)Cl_2(H_2O)_2]^+$ species (Fig. S7). For H_2L-Cu^{2+} complex the strong peak at 699.2 correspond to $Na[Cu_2(L)Cl_2]^+$ along with a weak peak at 717.3 corresponding to $Na[Cu_2(L)Cl_2(H_2O)]^+$ (Fig. S8) species supporting 1:2 complex formation for both zinc and copper complexes.

Cation sensing studies of H_2L

UV-Vis study

Receptor H_2L (20 μM) shows a strong absorbance band at 344 nm, and at 238 nm in 1:1, v/v CH_3CN:H_2O using HEPES buffered solution at pH=7.2. Gradual addition of Zn^{2+} (40 μM) shows a decrease in absorbance intensity at 344 nm with the appearance of a new absorption band at 265 nm (Fig. 1). Formation of this new band at 265 nm indicates the co-ordination of the receptor to Zn^{2+}. Again, on gradual addition of Cu^{2+} (40 μM) formation of low energy band is observed at 459 nm along with a new absorption band at 270 nm supporting the coordination of Cu^{2+} to the receptor (Fig. 2). UV-Vis spectrum of H_2L is also studied in presence of other metals i,e, Na^+, K^+, Ca^{2+}, Mg^{2+}, Mn^{2+}, Fe^{3+}, Cr^{3+}, Co^{2+}, Ni^{2+}, Al^{3+}, Cd^{2+} and Hg^{2+} but no significant changes are observed except for Hg^{2+} and Ni^{2+} (Fig. S9).

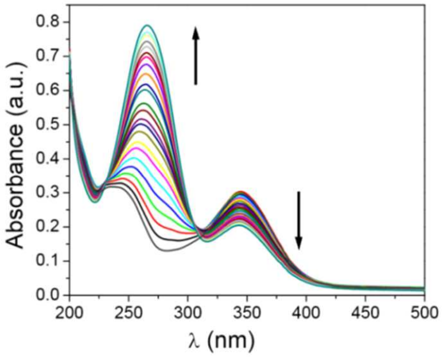

Fig. 1. Change in UV-Vis spectrum of H_2L (20 μM) upon gradual addition of Zn^{2+} (40 μM) in 1:1, v/v CH_3CN:H_2O

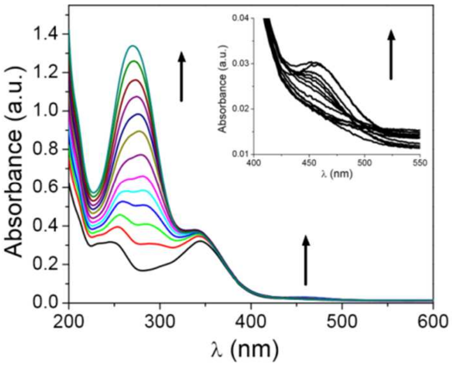

Fig. 2. Change in UV-Vis spectrum of H_2L (20 μM) upon gradual addition of Cu^{2+} (40 μM) in 1:1, v/v $CH_3CN:H_2O$

Fluorescence study

In the absence of metal ions the emission spectrum of the synthesized chemosensor H_2L shows a band with moderate emission intensity and maxima (F_0) at 484 nm ($\lambda_{excitation}$, 344 nm). The fluorescence quantum yield (ϕ = 0.012) is very poor. Gradual addition of Zn^{2+} to the above solution shows fluorescence enhancement by 6 fold (ϕ = 0.058) and the maxima at 484 nm vanished with the formation of new emission maxima at 466 nm (Fig. 3). This blue shift of 18 nm is due to co-ordination of the metal centre to the receptor. Thus the fluorescence enhancement reflects a strong selective OFF-ON fluorescent signaling property of H_2L for Zn^{2+}. While on addition of Cu^{2+} to the receptor solution quenching of emission intensity is observed by 7 folds, with the formation of a new emission maxima at 506 nm (Fig. 4). On addition of EDTA to the H_2L-Zn^{2+} solution, fluorescent intensity at 466 nm gradually decreases and the emission band at 484 nm reappears (Fig. S10). Again, on addition of EDTA to H_2L-Cu^{2+}, emission intensity again increases and the emission maxima blue shifted from 506 nm to 484 nm (Fig. S11).

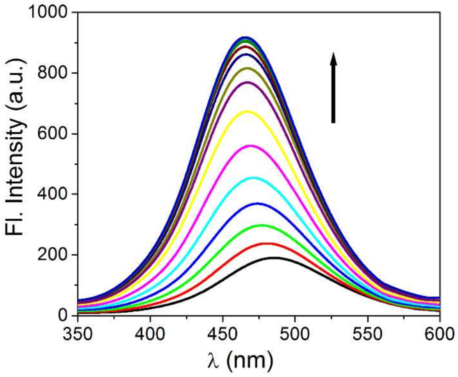

Fig. 3. Change in emission spectrum of H_2L (20 μM) upon gradual addition of Zn^{2+} (40 μM) in 1:1, v/v $CH_3CN:H_2O$.

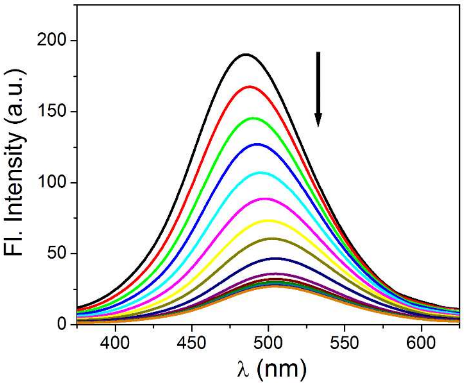

Fig. 4. Change in emission spectrum of H_2L (20 μM) upon gradual addition of Cu^{2+} (40 μM) in 1:1, v/v $CH_3CN:H_2O$.

Mole ratio plot obtained from fluorescence titration indicates that the receptor shows an increase in emission intensity till the ratio of Zn^{2+}:H_2L reaches ~2, after that there is hardly any increase in emission intensity (Fig. S12). Quenching of fluorescence intensity occurs till the ratio of Cu^{2+}:H_2L reaches 2 (Fig. S13). Jobs plot of emission intensity shows maxima in the plot corresponding to ~0.65 mole fraction for H_2L-Zn^{2+} complex (Fig. S14) and at ~0.66 mole fraction for H_2L with Cu^{2+}, reflecting 1:2 complex formation in both the cases (Fig. S15). From emission spectral change, limit of detection of the chemosensor for Zn^{2+} and Cu^{2+} are determined using the equation LOD = K × SD/S where 'SD' is the standard deviation of the blank solution and 'S' in the slope of the calibration curve (Fig. S16 and Fig. S17). The limit of detection for Zn^{2+} is 1.94×10^{-8} M from fluorescent titration while that of Cu^{2+} is found to be 1.87×10^{-9} M. This result clearly demonstrates that the chemosensor is highly efficient in sensing Zn^{2+} as well as Cu^{2+} even in very minute level. From fluorescent spectral titration the association constant of H_2L with Zn^{2+} and Cu^{2+} are found to be 1.8×10^{9} and 1.34×10^{10} respectively (Fig. S18 and Fig. S19).

Fluorescence emission intensity of H_2L (20 μM) is studied in presence of other metals i,e, Na^+, K^+, Ca^{2+}, Mg^{2+}, Mn^{2+}, Fe^{3+}, Cr^{3+}, Co^{2+}, Ni^{2+}, Al^{3+}, Cd^{2+} and Hg^{2+} (40 μM) in CH_3CN: H_2O (1:1, v/v, pH=7.2) but there is hardly any change in emission intensity of H_2L except in presence of Zn^{2+} and Cu^{2+} (Fig. S20).

In order to study the selectivity of H_2L for Zn^{2+} and Cu^{2+}, interference experiment is carried out by recording the emission intensity of H_2L (20 μM) in presence of other metal ions like Na^+, K^+, Ca^{2+}, Mg^{2+}, Mn^{2+}, Fe^{3+}, Cr^{3+}, Al^{3+}, Co^{2+}, Ni^{2+}, Cd^{2+} and Hg^{2+} (40 μM) before the addition of Zn^{2+} and Cu^{2+}. It is observed that the various competitive metal ions do not cause any significant interference both for Cu^{2+} and Zn^{2+}. The addition of Cu^{2+} to H_2L+Zn^{2+} causes sharp quenching of emission intensity as expected from association constant values. Thus H_2L basically shows an OFF-ON-OFF signally pattern in presence of Zn^{2+} and Cu^{2+}. To verify whether Cu^{2+} is responsible for the quenching of emission intensity, ascorbic acid is added to mask the effect of Cu^{2+} and the resulting solution shows an enhancement of fluorescence intensity as expected (Fig. 5).

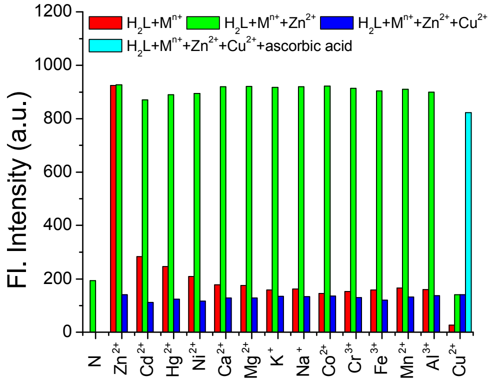

Fig. 5. Emission intensity of H_2L (20 µM) upon addition of Na^+, K^+, Ca^{2+}, Mg^{2+}, Mn^{2+}, Fe^{3+}, Cr^{3+}, Al^{3+}, Co^{2+}, Ni^{2+}, Cu^{2+}, Cd^{2+} and Hg^{2+} (40 µM) in CH_3CN:H_2O (1:1, v/v, pH=7.2) (red bars). Zn^{2+} (40 µM) in presence of other metal ions (green bars). Cu^{2+} and Zn^{2+} both 40 µM in presence of other metal ions (navy blue bars).

The effect of pH on the emission intensity of the receptor (H_2L) in absense and presence of Zn^{2+} and Cu^{2+} are studied. In case of H_2L there is hardly any change in fluorescence intensity in the pH range 1-4 (Fig. 6). Below pH 4 high fluorescence intensity is observed due to protonation of imine N and hydroxy O atoms preventing the excited state intramolecular proton transfer (ESIPT) process, which is responsible for the quenching of fluorescence intensity. On addition of 2 equivalents of Zn^{2+} the fluorescence intensity remains almost unchanged in the pH < 4, while there is a sharp increase in fluorescence intensity in the pH range 5-9 compared to H_2L. But, on further increase in pH fluorescence intensity drops drastically due to the formtion of $Zn(OH)_2$ at pH > 9. On addition of Cu^{2+}, quenching of fluorescent intensity of H_2L is significant in the pH range 4-9. Thus H_2L forms stable complex with Zn^{2+} and Cu^{2+} in the pH range of 5-9 hence the developed receptor H_2L can detect Zn^{2+} and Cu^{2+} in this pH range. However at low pH values (pH < 4) receptor tends to combine with protons and hence becomes ineffective in detection of Zn^{2+} and Cu^{2+}.

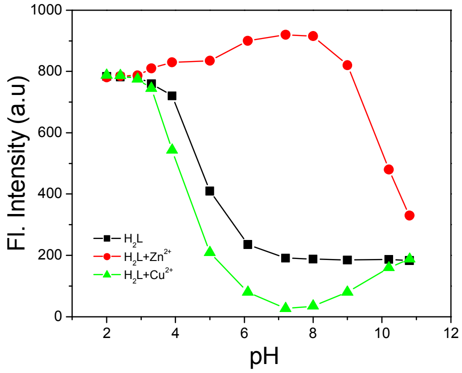

Fig. 6. pH dependence of fluorescence intensity of H_2L and its complexes with Zn^{2+} and Cu^{2+}.

Application as Logic function

The developed chemosensor H_2L can be utilised as a binary logic function with dual stimulating inputs as Zn^{2+} and Cu^{2+} and emission as output. As a result of coordination of H_2L with Zn^{2+}(IN1) a new emission band appears at 466 nm. Upon gradual addition of Cu^{2+}(IN2), the emission intensity of the band at 466 nm gets quenched. This preference of the receptor H_2L in binding with Cu^{2+} even in presence of Zn^{2+} is well explained from the binding constant values. Addition of Cu^{2+} alone to H_2L also results in quenching of emission intensity. The threshold value of fluoresence intensity is taken to be 190. OUT = 0 when intensity is less than 190; OUT = 1 when intensity is higher than 190. Now OUT = 1 only when Zn^{2+} is present alone. Actually it represents an AND gate with an inverter[28] in one of its input. Thus the emission change at 466 nm with Zn^{2+} as well as Cu^{2+} (with an invertor) as inputs can be interpretated as a monomolecular circuit showing an INHIBIT logic function[22] (Fig. 7).

Input		Output
IN1	IN2	OUT
Zn^{2+}	Cu^{2+}	Emission at 466 nm
0	0	0
0	1	0
1	0	1
1	1	0

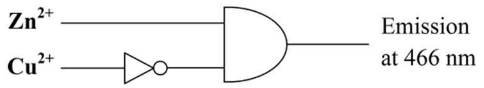

Fig. 7. Truth table and the monomolecular circuit based on Zn^{2+} and Cu^{2+}.

INPUT		OUTPUT
IN1	IN2	OUT
Zn^{2+}	EDTA	Emission at 466 nm
0	0	0
0	1	0
1	0	1
1	1	0
INPUT		OUTPUT
IN1	IN2	OUT
Cu^{2+}	EDTA	Emission at 484 nm
0	0	1
0	1	1
1	0	0
1	1	1

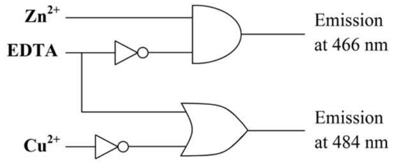

Fig. 8. Truth table and the monomolecular circuit based on Zn^{2+} with EDTA and EDTA with Cu^{2+}.

When EDTA (40 μM) is added to the H_2L-Zn^{2+} complex the solution shows a decrease of emission intensity and the band at 466 nm is disappeared, suggesting that the receptor H_2L has again returned to its free form. However in the absence of Zn^{2+}, EDTA does not have any effect on the emission intensity of the receptor H_2L (Fig. 8). Thus with two chemical inputs as Zn^{2+} and EDTA, H_2L functions as an AND gate with an inverter in the EDTA input by monitoring the emission output. This function can be interpreted as a monomolecular circuit showing an INHIBIT logic function. On the other hand when EDTA is added to the H_2L-Cu^{2+} solution, an obvious enhancement of fluoresence intensity is observed due to complex formation of EDTA with Cu^{2+} making the receptor free. Thus the emission intensity value at 484 nm is low only when Cu^{2+} is present. When Cu^{2+} is present along with EDTA the emission intensity at 484 nm is high. Thus it actually represents an OR with an inverter in one of its input which is also called an IMPLICATION logic gate.[29]

Electronic structure and sensing mechanism

To interpret the electronic structure of H_2L geometry optimization has been performed by DFT/B3LYP method for keto and enol forms in singlet ground state (S_0) (Scheme 2). The energy calculation in S_0 state reveals that the keto form is more stable by 8.025 kcal/mol than the corresponding enol form which is consistent with the X-ray structure of this type of molecules.[30] The geometry of H_2L-Zn^{2+} and H_2L-Cu^{2+} have been optimized and the energy minimized structures are shown in Fig. S21 and Fig. S22 respectively. In the complexes the chemosensor H_2L binds to Zn^{2+} and Cu^{2+} through phenolic-O atom and imine-N. Contour plots of some selected molecular orbitals of H_2L and its complexes with Zn^{2+} and Cu^{2+} are shown in Figs. S23-25.

To interpret the changes in electronic spectra TDDFT calculation by DFT/B3LYP/CPCM method has been carried out in acetonitrile. The intense band at 338 nm for chemosensor H_2L corresponds to HOMO → LUMO transition (Table S1). In H_2L-Zn^{2+} the intense HOMO → LUMO transition is observed at 340 nm having ILCT character. For H_2L-Cu^{2+} the very weak transition at 482 nm corresponds to ligand to metal charge transfer transition (LMCT) along with a strong transition at 359 nm corresponding to HOMO-1(β) → LUMO+2(β) transition has been observed.

The chemosensor H_2L shows a weak emission band centered around 484 nm. Upon gradual addition of Zn^{2+}, there is an enhancement of fluorescence intensity and a new emission band appears at 466 nm. To interprete whether the excited state intramolecular proton transfer (ESIPT)[31] is responsible for the quenching of fluorescence intensity for H_2L, theoretical calculations are carried out. The possible intramolecular proton transfer process in ground (S_0) state has been considered (Scheme 2) and there is only 8.025 kcal/mol of energy difference between the two forms. So, the hydrogen transfer takes place easily resulting in quenching of fluorescence for H_2L. On coordination with Zn^{2+} this ESIPT process is inhibited resulting in fluorescence intensity enhancement. However, the significant quenching of fluorescene intensity of H_2L upon addition of Cu^{2+} is expected due to the paramagnetic nature of Cu^{2+} ion.[32]

Experimental

Material and methods

4-Hydroxycoumarin and 1,4-Diaminobenzene were purchased from Aldrich. All other organic chemicals and inorganic salts were available from commercial suppliers and used without further purification.

Elemental analysis was carried out in a 2400 Series-II CHN analyzer, Perkin Elmer, USA. HRMS mass spectra were recorded on Waters (Xevo G2 Q-TOF) mass spectrometer. Infrared spectra were taken on a RX-1 Perkin Elmer spectrophotometer with samples prepared as KBr pellets. Electronic spectral studies were performed on a Perkin Elmer Lambda 25 spectrophotometer. Luminescence property was measured using Perkin Elmer LS 55 fluorescence spectrophotometer at room temperature (298 K). NMR spectra were recorded using a Bruker (AC) 300 MHz FTNMR spectrometer in $CDCl_3$.

The luminescence quantum yield was determined using carbazole as reference with a known ϕ_R of 0.42 in MeCN. The complex and the reference dye were excited at the same wavelength, maintaining nearly equal absorbance (~0.1), and the emission spectra were recorded. The area of the emission spectrum was integrated using the software available in the instrument and the quantum yield is calculated according to the following equation:

$$\phi_S/\phi_R = [A_S / A_R] \times [(Abs)_R /(Abs)_S] \times [\eta_S^2/\eta_R^2].$$

Here, ϕ_S and ϕ_R are the luminescence quantum yields of the sample and reference, respectively. A_S and A_R are the area under the emission spectra of the sample and the reference respectively, $(Abs)_S$ and $(Abs)_R$ are the respective optical densities of the sample and the reference solution at the wavelength of excitation, and η_S and η_R are the values of refractive index for the respective solvent used for the sample and reference.

Synthesis of the receptor (H_2L)

3-Acetyl-4-hydroxy-2H-chromen-2-one (L)[33] (0.204 g, 1.0 mmol) and 1,4-Diaminobenzene (0.054 g, 0.5 mmol) were refluxed for 6 hours in methanolic medium. Solvent was evaporated under reduced pressure and then dissolved in dichoromethane which is then further subjected to silica gel (60-120 mesh) column chromatographic separation. The desired light yellow solid product was obtained by elution with 35% ethylacetate: pet-ether (v/v) mixture. Yield was, 0.399 g, 83%.

Anal. Calc. for $C_{28}H_{20}N_2O_6$ (H_2L): Calc. (%) C 69.99, H 4.20, N 5.83. Found (%), C 69.03, H 4.01, N 5.21. IR data (KBr, cm^{-1}): 1698 υ(lactone C=O); 1610 υ(keto C=O), 1547 υ(C=C). ^1H NMR data ($CDCl_3$, 300 MHz):δ 15.45 (2H, s), 8.10 (2H, d, J= 7.4 Hz), 7.60 (2H, t, J= 7.2 Hz), 7.38 (4H, s), 7.27-7.32 (4H, m), 2.79 (6H, s).

General method for UV-Vis and fluorescence titration

Stock solution of the receptor H_2L (10 μM) in [(CH_3CN/H_2O), 1:1, v/v] (at 25°C) using HEPES buffered solution at pH=7.2 was prepared. The solution of the guest cations using their chloride salts in the order of 100 μM were prepared in deionised water. Solutions of various concentrations containing host and increasing concentrations of cations were prepared separately. The spectra of these solutions were recorded by means of UV-Vis methods. EDTA solution of 100 μM was added to the same solution where Zn^{2+} and Cu^{2+} were added gradually to H_2L and emission spectra recorded. The spectra of all these solutions were also recorded by means of fluorescence methods.

Job's plot by fluorescence method

A series of solutions containing H_2L (10 μM), $ZnCl_2$ and $CuCl_2$ (10 μM) were prepared in such a manner that the sum of the total metal ion and H_2L volume remained constant (4 ml). $CH_3CN:H_2O$ (1:1, v/v) was used as solvent at pH 7.2 using HEPES buffer. Job's plots were drawn by plotting ΔF versus mole fraction of Zn^{2+} and Cu^{2+}.

Computational method

All calculations were carried out at the B3LYP[34] level using Gaussian 09 software package.[35] The 6-31G(d,p) basis set was assigned for the elements except for zinc and copper. The LANL2DZ basis set, with an effective core potential for Zn and Cu, was used.[36] Vertical electronic excitations based on B3LYP optimized geometries were computed using the time-dependent density functional theory (TDDFT) formalism[37] in acetonitrile using conductor-like polarizable continuum model (CPCM).[38]

Conclusions

Thus we have successfully developed a new coumarin based chemosensor for the selective dual sensing of Cu^{2+} and Zn^{2+} over other metal ions. The receptor H_2L shows about 6 fold increase in fluorescent intensity upon addition of Zn^{2+} and also exhibits quenching of emission intensity upon addition of Cu^{2+} without the interference of other metal ions present in solution. It exhibits two sets of integrated logic gates: (a) one INHIBIT logic gate with Zn^{2+} and Cu^{2+} or Zn^{2+} and EDTA as chemical inputs (b) one IMPLICATION logic gate with Cu^{2+} and EDTA as chemical inputs. We belief that in near future, our designed chemosensor H_2L will lead to several important openings in the synthesis of other important chemosensors with additional application in biological systems.

Acknowledgement

Financial supports received from the Department of Science and Technology, New Delhi, India (No. SB/EMEQ–242/2013) is gratefully acknowledged. D. Sarkar and A. K. Pramanik are thankful to CSIR, New Delhi, India, for their fellowships.

Notes and references

[a] *Department of Chemistry, Jadavpur University, Kolkata-700032, India*
E-mail: tkmondal@chemistry.jdvu.ac.in

†Electronic Supplementary Information (ESI) available: [Association constant determination, detection limit determination, ^1H NMR, HRMS, UV-Vis titration spectra of HL with different metal ions etc.].

.

1 (a) E.L. Que, D.W. Domaille, C.J. Chang, *Chem. Rev.*, 2008, **108**, 1517; (b) M. Li, H. Ge, R.L. Arrowsmith, V. Mirabello, S.W. Botchway, W. Zhu, S.I. Pascu, T.D. James, *Chem. Commun.*, 2014, **50**, 11806.

2 (a) Z. Dai, J.W. Canary, *New J. Chem.*, 2007, **31**, 1708; (b) K. Jobe, C.H. Brennan, M. Motevalli, S.M. Goldup, M. Watkinson, *Chem. Commun.*, 2011, **47**, 6036.

3 H. Scherz, E. Kirchhoff, *J. Food Compost. Anal.*, 2006, **19**, 420.

4 P.C. Bull, G.R. Thomas, J.M. Rommens, J.R. Forbes, D.W. Cox, *Nat. Genet.*, 1993, **5**, 327.

5 (a) P. Li, X. Duan, Z. Chen, Y. Liu, T. Xie, L. Fang, X. Li, M. Yin, B. Tang, *Chem. Commun.*, 2011, **47**, 7755; (b) N. J. Robinson, D. R. Winge, *Biochemistry*, 2010, **79**, 537.

6 T. Finkel, M. Serrano, M. A. Blasco, *Nature*, 2007, **448**, 767.

7 Q. Zou, X. Li, J. Zhang, J. Zhou, B. Sun, H. Tian, *Chem. Commun.*, 2012, **48**, 2095.

8 Z.Q. Guo, W.-Q. Chen, X.-M. Duan, *Org. Lett.*, 2010, **12**, 2202.

9 S. Dalapati, S. Jana, M. A. Alam, N. Guchhait, *Sens. Actuators, B*, 2011, **160**, 1106.

10 C. Vulpe, B. Levinson, S. Whitney, S. Packman, J. Gitschier, *Nat. Genet.*, 1993, **3**, 7.

11 S.H. Hahn, M.S. Tanner, D.M. Danke, W.A. Gahl, *Biochem. Mol. Med.*, 1995, **54**, 142.

12 (a) K. Shen, X. Yang, Y. Cheng and C. Zhu, *Tetrahedron*, 2012, **68**, 5719; (b) L. Zhao, L. Yang, C. He, J. Wang, C. Duan, *Dalton Trans.*, 2014, **43**, 335; (c) T. Sakamoto, A. Ojida, I. Hamachi, *Chem. Commun.*, 2009, 141; (d) Z. Liu, W. He, Z. Guo, *Chem. Soc. Rev.*, 2013, **42**, 1568; (e) D. Buccella, J. A. Horowitz, S. J. Lippard, *J. Am. Chem. Soc.*, 2011, **133**, 4101.

13 (a) D. Sarkar, A.K. Pramanik, T.K. Mondal, *RSC Adv.*, 2014, **4**, 25341; (b) D. Sarkar, A.K. Pramanik, T.K. Mondal, *J. Lumin.*, 2014, **146**, 480; (c) S.S. Mati, S. Chall, S. Konar, S. Rakshit, S.C. Bhattacharya, *Sens. Actuators, B*, 2014, **201**, 204; (d) S. Goswami, A.K. Das, K. Aich, A. Manna, S. Maity, K. Khanra, N. Bhattacharyya, *Analyst*, 2013, **138**, 4593.

14 (a) P. Kaur, S. Kaur, K. Singh, P.R. Sharma, T. Kaur, *Dalton Trans.*, 2011, **40**, 10818; (b) J. Huang, M. Liu, X. Ma, Q. Dong, B. Ye, W. Wang, W. Zeng, *RSC Adv.*, 2014, **4**, 22964.

15 (a) R. Azadbakht, H. Keypour, H. A. Rudbari, A. H. Mohammad Zaheri, S. Menati, *J. Lumin.*, 2012, **132**, 1860; (b) H. Song, S. Rajendiran, E. Koo, B. K. Min, S. K. Jeong, T. D. Thangadurai, S. Yoon, *J. Lumin.*, 2012, **132**, 3089; (c) S. Kotha, D. Goyal, S. Banerjee, A. Datta, *Analyst*, 2012, **137**, 2871.

16 (a) R. Alam, T. Mistri, A. Katarkar, K. Chaudhuri, S.K. Mandal, A.R. Khuda-Bukhsh, K.K. Das, M. Ali, *Analyst*, 2014, **139**, 4022; (b) M. Shellaiah, Y.-H. Wu, H.-C. Lin, *Analyst*, 2013, **138**, 2931; (c) H.N. Kim, W.X. Ren, J.S. Kim, J. Yoon, *Chem. Soc. Rev.*, 2010, **39**, 3102; (d) A. Liu, L. Yang, Z. Zhang, Z. Zhang, D. Xu, *Dyes Pigments*, 2013, **99**, 472; (e) J. Q. Ang, B.T.T. Nguyen, C.-S. Toh, *Sens. Actuators, B*, 2011, **157**, 417; (f) S. Goswami, S. Das, K. Aich, D. Sarkar, T.K. Mondal, *Tetrahedron Lett.*, 2013, **54**, 6892; (g) S. Goswami, S. Paul, A. Manna, *RSC. Adv.*, 2013, **3**, 25079.

17 K. Szacilowski, *Chem. Rev.*, 2008, **108**, 3481.

18 (a) X. Chen, Z. Li, Y. Xiang, A. Tong, *Tetrahedron Lett.*, 2008, **49** 4697; (b) U. Pischel, B. Heller, *New J. Chem.*, 2008, **32**, 395; (c) T. Gupta, M.E. van der Boom, *Angew. Chem. Int. Ed.*, 2008, **47**, 5322.

19 (a) A.P. de Silva, N.D. McClenaghan, *Chem. Eur. J.*, 2004, **10**, 574; (b) U. Pischel, *Angew. Chem. Int. Ed.*, 2007, **46**, 4026.

20 K. Rurack, C. Trieflinger, A. Koval'chuck, J. Daub, *Chem. Eur. J.*, 2007, **13**, 8998.

21 (a) L. Zhao, D. Sui, J. Chai, Y. Wang, S. Jiang, *J. Phys. Chem.B.*, 2006, **110**, 24299; (b) L. Zhao, Q. Hou, D. Sui, Y. Wang, S. Jiang, *Spectrochim. Acta Part A*, 2007, **67**, 1120; (c) L. Zhao, S. Wang, Y. Wu, Q. Hou, Y. Wang, S. Jiang, *J. Phys. Chem. C*, 2007, **111**, 18387.

22 D. Sarkar, A. Pramanik, S. Biswas, P. Karmakar, T. K. Mondal, *RSC Adv.*, 2014, **4**, 30666.

23 (a) D. Ray, P.K. Bharadwaj, *Inorg. Chem.*, 2008, **47**, 2252; (b) N.C. Lim, J.V. Schuster, M.C. Porto, M.A. Tanudra, L.L. Yao, H.C. Freake, C. Bruckner, *Inorg. Chem.*, 2005, **44**, 2018; (c) H.E. Katerinopoulos, *Curr. Pharm. Des.*, 2004, **10**, 3835.

24 (a) M. Suresh, A. Das, *Tetrahedron Lett.*, 2009, **50**, 5808; (b) L. Cao, C. Jia, Y. Huang, Q. Zhang, N. Wang, Y. Xue, D. Du, *Tetrahedron Lett.*, 2014, **55**, 4062; (c) H. A. El-Shekheby, A. H. Mangood, S. M.

Hamza, A. S. Al-Kady, E. M. Ebeid, *Luminescence*, 2014, **29**, 158; (d) J. Hou, B. Liu, K. Li, K. Yu, M. Wu, X. Yu, *Talanta,*2013, **116**, 434; (e) H. Wang, Y. Feng, S. Meng, J. Chem. Res., 2012, **36**, 587; (f) J. Wu, R. Sheng, W. Liu, P. Wang, H. Zhang, J. Ma, *Tetrahedron*, 2012, **68**, 5458; (g) N. Chattopadhyay, A. Mallick, S. Sengupta, J. *Photoch. Photobio. A*, 2006, **177**, 55.

25 S. Wang, G. Men, L. Zhao, Q. Hou, S. Jiang, *Sens. Actuators, B,* 2010, **145**, 826.

26 Y. Liu, Q. Fei, H. Shan, M. Cui, Q. Liu, G. Feng, Y. Huan, *Analyst*, 2014, **139**, 1868.

27 L. Qua, C. Yina, F. Huob, J. Chaob, Y. Zhang, F. Cheng, *Sens. Actuators, B*, 2014, **191**, 158.

28 M.V. López, M.E. Vázquez, C. Gómez-Reino, R. Pedrido, M.R. Bermejo, *New J. Chem.*, 2008, **32**, 1473.

29 (a) A.P. de Silva, N.D. McClenaghan, *Chem. Eur. J.* 2002, **8**, 4935; (b) Y. Fu, Q. Feng, X. Jiang, H. Xu, M. Li, S. Zang, *Dalton Trans.*, 2014, **43**, 5815; (c) D. C. Magri, M. C. Fava, C. J. Mallia, Chem. Commun., 2014, **50**, 1009; (d) S. Wang, G. Men, L. Zhao, Q. Hou, S. Jiang, *Sens. Actuators, B*, 2010, **145**, 826.

30 (a) A. Brahmia, T.B. Ayed, R.B. Hassen, *Acta Crystallogr., Sect. E: Struct. Rep. Online*, 2013, **69**, o1296; (b) T. Shibahara, M. Takahashi, A. Maekawa, H. Takagi, *Acta Crystallogr., Sect. E: Struct. Rep. Online*, 2010, **66**, o429.

31 (a) A.J. Moghadam, R.Omidyan,. V. Mirkhani, . G. Azimi, *J. Phys. Chem. A*, 2013, **117**, 718; (b) Z. Wang, D. M. Friedrich, C. C. Ainsworth, S. L. Hemmer, A. G. Joly, M. R. Beversluis, *J. Phys. Chem. A*, 2001, **105**, 942; (c) I. Presiado, Y. Erez, R. Gepshtein and D. Huppert, *J. Phys. Chem. C,* 2010, **114**, 3634; (d) F. Wua, L. Ma, S. Zhanga, Y. Genga, J. Lüa, X. Chenga, *Chem. Phys. Lett.*, 2012, **141**, 519.

32 (a) K. M. K. Swamy, S. K. Ko, S. K. Kwon, H. N. Lee, C. Mao, J. M. Kim, K. H. Lee, J. Kim, I. Shin, J. Yoon, *Chem. Commun.*, 2008, 5915; (b) H. S. Jung, P. S. Kwon, J. W. Lee, J. I. Kim, C. S. Hong, J. W. Kim, S. Yan, J. Y. Lee, J. H. Lee, T. Joo, J. S. Kim, *J. Am. Chem. Soc.*, 2009, **131**, 2008.

33 N. Hamdi, C. Fischmeister, M.C. Puerta, P. Valerga, *Med. Chem. Res.*, 2011, **20**, 522.

34 (a) A.D. Becke, *J. Chem. Phys.,* 1993, **98**, 5648; (b) C. Lee, W. Yang, R. G. Parr, *Phys. Rev. B*, 1988, **37**, 785; (c) D. Andrae, U. Haeussermann, M. Dolg, H. Stoll and H. Preuss, *Theor. Chim. Acta*, 1990, **77**, 123.

35 Gaussian 09, Revision D.01, M. J. Frisch, G. W. Trucks, H. B. Schlegel, G. E. Scuseria, M. A. Robb, J. R. Cheeseman, G. Scalmani, V. Barone, B. Mennucci, G. A. Petersson, H. Nakatsuji, M. Caricato, X. Li, H. P. Hratchian, A. F. Izmaylov, J. Bloino, G. Zheng, J. L. Sonnenberg, M. Hada, M. Ehara, K. Toyota, R. Fukuda, J. Hasegawa, M. Ishida, T. Nakajima, Y. Honda, O. Kitao, H. Nakai, T. Vreven, J. A. Montgomery, Jr., J. E. Peralta, F. Ogliaro, M. Bearpark, J. J. Heyd, E. Brothers, K. N. Kudin, V. N. Staroverov, R. Kobayashi, J. Normand, K. Raghavachari, A. Rendell, J. C. Burant, S. S. Iyengar, J. Tomasi, M. Cossi, N. Rega, J. M. Millam, M. Klene, J. E. Knox, J. B. Cross, V. Bakken, C. Adamo, J. Jaramillo, R. Gomperts, R. E. Stratmann, O. Yazyev, A. J. Austin, R. Cammi, C. Pomelli, J. W. Ochterski, R. L. Martin, K. Morokuma, V. G. Zakrzewski, G. A. Voth, P. Salvador, J. J. Dannenberg, S. Dapprich, A. D. Daniels, Ö. Farkas, J. B. Foresman, J. V. Ortiz, J. Cioslowski, and D. J. Fox, Gaussian, Inc., Wallingford CT, 2009.

36 P.J. Hay, W.R. Wadt, *J. Chem. Phys*., 1985, **82,** 299.

37 (a) R. Bauernschmitt, R. Ahlrichs, *Chem. Phys. Lett*., 1996, **256**, 454; (b) R.E. Stratmann, G.E. Scuseria, M.J. Frisch, *J. Chem. Phys*., 1998, **109**, 8218; (c) M.E. Casida, C. Jamorski, K.C. Casida, D.R. Salahub, *J. Chem. Phys.,*1998, **108,** 4439.

38 (a) V. Barone, M. Cossi, *J. Phys. Chem. A*, 1998, **102**, 1995; (b) M. Cossi, V. Barone, *J. Chem. Phys.*, 2001, **115**, 4708; (c) M. Cossi, N. Rega, G. Scalmani, V. Barone, *J. Comput. Chem.*, 2003, **24,** 669.